EFFECT OF A SURFACE ROUGHNESS ON THE CRACK DRIVING FORCE OF PHYSICALLY SHORT STATIONARY CRACK – NUMERICAL SIMULATION
Michal Kráčalík

EFFECT OF A SURFACE ROUGHNESS ON THE CRACK DRIVING FORCE OF PHYSICALLY SHORT STATIONARY CRACK – NUMERICAL SIMULATION

Michal Kráčalík

Untere Hauptstraße 48/5, 2424 Zurndorf, Austria, michal.kracalik@gmail.com

Abstract: The surface roughness, residual stresses and microstructure are main parameters that cause surface crack initiation in theoretically porous free materials. Hence, the effect of the surface roughness on the crack driving force is investigated regarding physically short stationary cracks in this paper. FE simulations show that mechanically short stationary cracks have practically zero crack driving force and the orientation of the crack driving force will not support crack growth. The crack driving force follows the material deformation around the crack tip in the opposite direction as is the supposed crack extension.

1 Introduction

Real surfaces are never really flat. Chemical, electrochemical treatment and generally production technology affect surface roughness [1] [2] [3] [4]. Surface roughness influences crack initiation and fatigue life of various materials under various mechanical and thermal loading conditions [5] [6] [7] [8] [9] [10]. From the mechanical point of view, surface roughness acts generally as a stress concentrator and influences fatigue life [11] [12] [13] [14]. From the fracture mechanics point of view, physically short cracks (further denotes only as short cracks) are substantially larger than the scale of the local plastic deformation with characteristic microstructural dimension usually smaller (in lengths) than 1-2 mm and they grow faster than physically long cracks (further only as long cracks) [15] – the threshold value is smaller compared to long crack [15] [16] [17].

The effect of the surface roughness on short crack is investigated by means of FE simulation. The simple plane stress FE Model evaluates crack driving force for three crack lengths and arithmetic surface roughness Ra. The FE Model does not take into account any crack closure mechanisms (review can be found in [18]). However, crack closure mechanism is not present, if crack starts to grow from small processing or metallurgical defects in form of pre-existing crack-like defect [19]. Explicitly is assumed that long cracks are not influenced by surface roughness and they are not investigated in the paper; the crack is modelled as a stationary crack (no crack extension is simulated).

Crack driving force concept is introduced in Chapter 2. FE Model is described in Chapter 3, results are presented in Chapter 4 and discussed in Chapter 5.

2 Crack driving force

The J-Integral is a crack driving force concept valid for nonlinear (and linear) material behaviour subjected monotonic loading; is defined as a path independent line integral and equal to the energy release rate [16]:

$$J = \int_{\Gamma} \left(w dy - T_i \frac{\partial u_i}{\partial x} ds \right), \qquad (1)$$

where w is the strain energy density, T_i is the traction vector (component), u_i is the displacement vector (component) and ds is length increment on the contour Γ.

3 FE Model

The FE plane stress model has a size of 100x100x10 μm. Mesh element size 1 μm is used in the whole model. The fix boundary conditions are prescribed in the bottom points in the FE model, see Figure 1. The Force F with magnitude 0.01 N is prescribed to the points in upper part of the Model. Scheme of the FE model is shown in Figure 1.
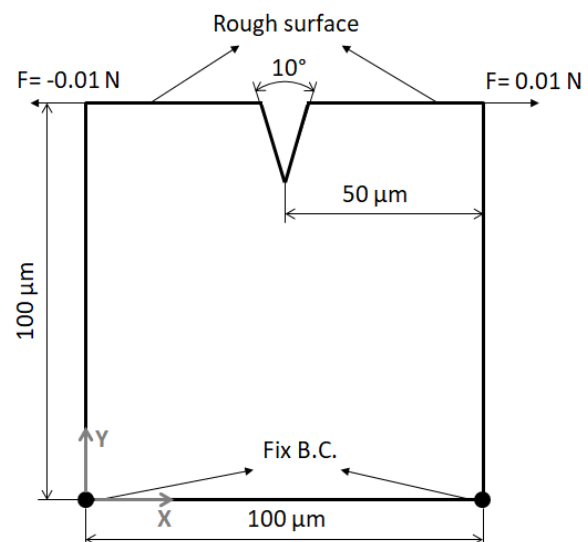

Figure 1 Scheme of the FE Model

EFFECT OF A SURFACE ROUGHNESS ON THE CRACK DRIVING FORCE OF PHYSICALLY SHORT STATIONARY CRACK – NUMERICAL SIMULATION
Michal Kráčalík

One straight crack with length of 10, 20, 30 µm is embedded to the upper surface in the model. The crack has a wedge like geometry with opening angle of 10°. The crack is located either in the middle of the upper surface (X=50 µm) assuming a flat surface or approximately in the middle of the upper surface, see "Crack initiation" in Figure 2.

The arithmetic mean roughness Ra is modelled by the probability density function with the normal distribution in Python 3.6 (numpy library) with mean distribution of 3.2, 6.3 µm respectively; both with standard deviation 1 µm. The generated surface roughness is shown in Figure. 2. Generated points are imported to Ansys 16 and the rough surface is created.
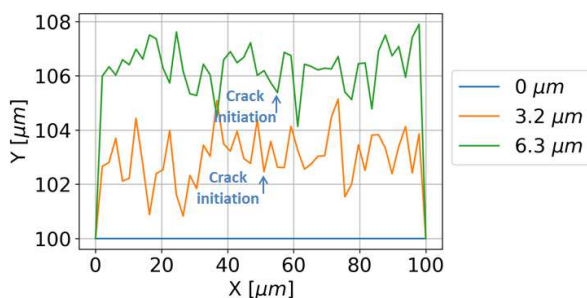

Figure 2 Arithmetic mean roughness Ra with marked crack initiation position. Crack initiation position is chosen approximately in the "roughness wedge" at the middle of the upper surface in order to reduce effect of the boundary condition in the FE model. Crack initiation on the flat surface (0 µm) is located at X position 50 µm.

A linear-elastic material model is used in the simulation with following parameters: Young's Modulus E=200 GPa, Poisson number ν=0.3. The local coordinate system of a crack is located at the crack tip. Mode I component (in the Y direction in global coordinate system) is evaluated.

4 Results
4.1   Numerical investigation
Figure 3 shows contour dependency of the computed crack driving force (J-Integral) for three crack lengths 10, 20, 30 µm. Flat surfaces is assumed in the simulations. Results show stabilization of the computed crack driving force since 3rd contour. Crack length of 10 µm demonstrates other trends of the computed crack driving force for 1st integration contour than crack lengths 20 and 30 µm, see Figure 3. The reason is irregular mesh for crack length of 10 µm created by automated mesh generation (soft meshing) in FE Software that influence results significantly; the mesh around other crack lengths is meshed regularly. Generally, it is not recommended usage of crack tip (1st integration contour) as a valid integration contour due to numerical accuracy [16]. The 3rd integration contour will be used in the further investigations.
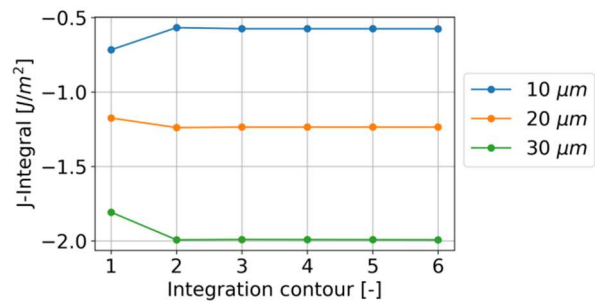

Figure 3 Contour dependency of the computed crack driving force (J-Integral) for three crack lengths (10, 20, 30 µm). Flat surface is assumed. 3rd and higher contour is numerically independent and will be used in further simulations.

The computed values are negative (related to the local coordinate system of a crack) - cracks have no tendency to growth. This phenomenon will be discussed in the next chapter.

4.2   Effect of the crack length and the surface roughness on the crack driving force
Figure 4 shows effect of the crack length and surface roughness on the crack driving force. Results for the 3rd integration contour are plotted. The longest crack (30 µm) has highest negative values – the crack has the smallest tendency to grow. The shortest crack (10 µm) has the "highest tendency to grow" – the values are in every investigated case negative. The material motion to the crack tip was observed in [20] but the context of the paper differs significantly from the presented one. The displacement field (material motion) will be discussed later in Chapter 4.3.
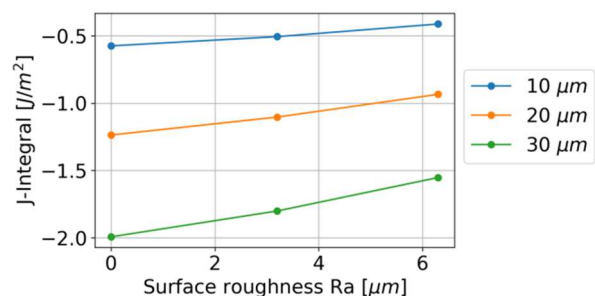

Figure 4 3rd integration contour of J-integral for three crack lengths (10, 20, 30 µm) over surface roughness Ra.

The surface roughness shifts negative values of crack driving force toward positive values but values are still negative (Figure 4). The computed results confirm observations that the crack propagation (and initiation) is supported by surface roughness [9] [12] [21] [22]. However, the continuum mechanics approach used in this paper has to be critically assessed regarding to short (stationary) crack, micromechanical approach and threshold values; more details can be found for instance in the review paper [23].

Acta Simulatio – International Scientific Journal about Simulation
Volume: 4 2018 Issue: 4 Pages: 7-10 ISSN 1339-9640

EFFECT OF A SURFACE ROUGHNESS ON THE CRACK DRIVING FORCE OF PHYSICALLY SHORT
STATIONARY CRACK – NUMERICAL SIMULATION
Michal Kráčalík

4.3   Displacement and stress field around the crack

Figure 5a shows displacement U_Y with marked non-deformed geometry and Figure 5b shows scoped perpendicular stresses on the crack S_{XX}. Scale 100 is used in Figure 5. The results are shown for crack length of 20 µm and Ra=3.2 µm.

The crack is moved in the up (Y) direction (a) and opened in crack Mode I (b). The maximum S_{XX} stresses are approximately 400 MPa around the crack tip (with prescribed force 0.01 N in the FE model).
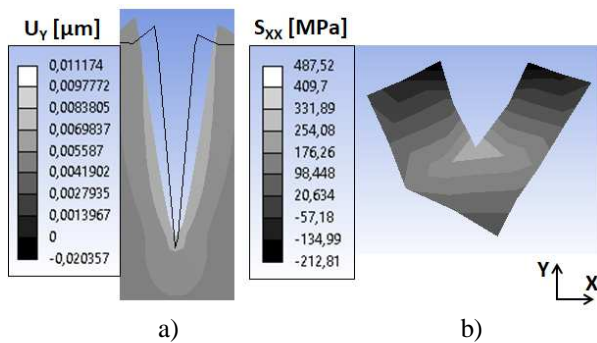

Figure 5 Displacement U_Y with marked non-deformed geometry (a). The crack is moved in the up (Y) direction. Scoped perpendicular stresses on the crack S_{XX} (b). The maximum stresses are approximately 400 MPa around the crack tip; the crack is opened – crack Mode I. The results are plotted for crack lengths of 20 µm and Ra=3.2 µm. The global coordinate system is used for plotting the result and scale 100 is used in the Figure.

The relationship between the J-integral and the displacement U_Y is plotted in Figure 6. U_Y is taken from the crack tip node. The deepest crack tip (30 µm) shows highest displacement upward and corresponding J-integral has the highest retardation tendency on the crack. Surface roughness decreases displacement upward and retardation effect on the crack decreases.

Figure 6 3rd integration contour of the J-integral (solid line) and the displacement U_Y (dashed line) for three crack lengths (10, 20, 30 µm) over surface roughness Ra. U_Y is taken from the crack tip node. The deepest crack tip (30 µm) shows highest displacement upwards and corresponding J-integral has the highest retardation tendency on the crack. Surface roughness decreases displacement upward and retardation effect on the crack decreases.
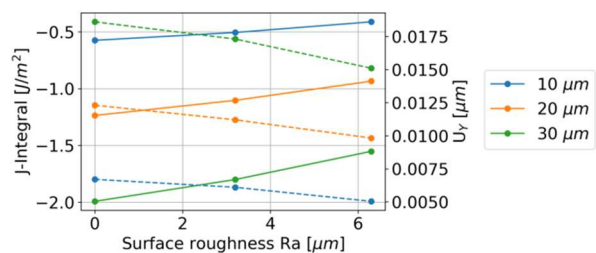
5   Discussion

The computed results are in accordance with two well observed phenomes. Firstly, the shortest crack (10 µm) would grow faster than longest cracks (20 and 30 µm) – the threshold value of small crack is smaller than longer cracks [15] [16] [17] [23] but clear distinction between microstructurally and physically small crack is not known. For instance, in [17] was for pearlitic steel chosen as the largest microstructural barrier 20 µm. This paper is focus only on physically short stationary cracks and the results should be assessed cautiously. Secondly, the high surface roughness leads to earlier crack initiation and smaller fatigue life than low surface roughness [9] [12] [21] [22] but this paper does not investigate crack initiation or fatigue life. Thus, the computed results are verified only indirectly.

Conclusions

The effect of a surface roughness on the crack driving force of stationary crack has been investigated in this paper. FE simulations show that crack driving force of physically short (stationary) crack follows material deformation and the surface roughness would support crack grow. This result is in accordance with experimental observations.

References

[1] KAJIKAWA, Y.: Roughness evolution during chemical vapor deposition, *Materials Chemistry and Physics,* Vol. 112, No. 2, pp. 311-318, 2008.
[2] BAEK, S.H., SHIM, H.-S., KIM, J.G., HUR, D.H.: Effect of chemical etching of fuel cladding surface on crud deposition behavior in simulated primary water of PWRs at 328 °C, *Annals of Nuclear Energy*, Vol. 116, No. June 2018, pp. 69-77, 2018.
[3] BONIN, L., CASTRO, C.C., VITRY, V., HANTSON A.-L., DELAUNOIS, F.: Optimization of electroless NiB deposition without stabilizer, based on surface roughness and plating rate, *Journal of Alloys and Compounds*, Vol. 767, No. October 2018, pp. 276-284, 2018.
[4] KRÁLIK, M., JERZ, V.: The Measurement of Residual Stresses in the Surface Layers of the Materials after Machining, *Materials Science Forum*, Vol. 919, No. April 2018, pp. 345-353, 5 2018.
[5] GALLO, P., BERTO, F.: Influence of surface roughness on high temperature fatigue strength and cracks initiation in 40CrMoV13.9 notched components, *Theoretical and Applied Fracture Mechanics,* Vol. 80, No. December 2015, pp. 226-234, 2015.
[6] LACERDA, J.C., MARTINS, G.D., SIGNORETTI, V.T., TEIXEIRA, R.L.P.: Evolution of the surface roughness of a low carbon steel subjected to fatigue, *International Journal of Fatigue,* Vol. 102, No. September 2017, pp. 143-148, 2017.

EFFECT OF A SURFACE ROUGHNESS ON THE CRACK DRIVING FORCE OF PHYSICALLY SHORT STATIONARY CRACK – NUMERICAL SIMULATION
Michal Kráčalík

[7] WANG, J., ZHANG, Y., SUN, Q., LIU, S., SHI, B., LU, H.: Giga-fatigue life prediction of FV520B-I with surface roughness, *Materials & Design*, Vol. 89, No. January 2016, pp. 1028-1034, 2016.

[8] MOLAEI, R., FATEMI, A., PHAN, N.: Significance of hot isostatic pressing (HIP) on multiaxial deformation and fatigue behaviors of additive manufactured Ti-6Al-4V including build orientation and surface roughness effects, *International Journal of Fatigue,* Vol. 117, No. December 2018, pp. 352-370, 2018.

[9] BAGEHORN, S., WEHR, J., MAIER, H.J.: Application of mechanical surface finishing processes for roughness reduction and fatigue improvement of additively manufactured Ti-6Al-4V parts, *International Journal of Fatigue*, Vol. 102, No. September 2017, pp. 135-142, 2017.

[10] HAGHSHENAS, A., KHONSARI, M.M.: Damage accumulation and crack initiation detection based on the evolution of surface roughness parameters, *International Journal of Fatigue*, Vol. 107, No. February 2018, pp. 130-144, 2018.

[11] JAVIDI, A., RIEGER, U., EICHLSEDER, W.: The effect of machining on the surface integrity and fatigue life, *International Journal of Fatigue*, Vol. 30, No. 10-11, pp. 2050-2055, 2008.

[12] DAI, W.B., YUAN, L.X., LI, C.Y., HE, D., JIA, D.W., ZHANG, Y.M.: The effect of surface roughness of the substrate on fatigue life of coated aluminum alloy by micro-arc oxidation, *Journal of Alloys and Compounds*, Vol. 765, No. October 2018, pp. 1018-1025, 2018.

[13] SKALLERUD, S.K.ÅS,B., TVEITEN, B.W.: Surface roughness characterization for fatigue life predictions using finite element analysis, *International Journal of Fatigue*, Vol. 30, pp. 2200-2209, 2008.

[14] LIU, G., HUANG, C., ZOU, B., WANG, X., LIU, Z.: Surface integrity and fatigue performance of 17-4PH stainless steel after cutting operations, *Surface and Coatings Technology,* Vol. 307, No. December 2016, pp. 182-189, 2016.

[15] MAIERHOFER, J., PIPPAN, R., GÄNSER, H.-P.: Modified NASGRO equation for physically short cracks, *International Journal of Fatigue*, Vol. 59, No. February 2014, pp. 200-207, 2014.

[16] ANDERSON, T.L., ANDERSON, T.L.: *Fracture Mechanics: Fundamentals and Applications,* 3rd ed., CRC Press, 2005.

[17] KOLITSCH, S., GÄNSER, H.-P., PIPPAN, R.: Determination of crack initiation and crack growth stress-life curves by fracture mechanics experiments and statistical analysis, *Procedia Structural Integrity*, Vol. 2, pp. 3026-3039, 2016.

[18] PIPPAN, R., HOHENWARTER, A.: Fatigue crack closure: a review of the physical phenomena, *Fatigue & Fracture of Engineering Materials & Structures*, Vol. 40, No. 4, pp. 471-495, 2017.

[19] MAIERHOFER, J., KOLITSCH, S., PIPPAN, R., GÄNSER, H.-P., MADIA, M., ZERBST, U.: The cyclic R-curve – Determination, problems, limitations and application, *Engineering Fracture Mechanics,* Vol. 198, No. July 2018, pp. 45-64, 2018.

[20] FISCHLSCHWEIGER, M., ECKER, W., PIPPAN, R.: Verification of a continuum mechanical explanation of plasticity-induced crack closure under plain strain conditions by means of finite element analysis, *Engineering Fracture Mechanics,* Vol. 96, No. December 2012, pp. 762-765, 2012.

[21] WU, D., YAO, C., ZHANG, D.: Surface characterization and fatigue evaluation in GH4169 superalloy: Comparing results after finish turning; shot peening and surface polishing treatments, *International Journal of Fatigue*, Vol. 113, pp. 222-235, 2018.

[22] SHAHZAD, M., CHAUSSUMIER, M., CHIERAGATTI, R., MABRU, C., REZAI-ARIA, F.: Surface characterization and influence of anodizing process on fatigue life of Al 7050 alloy, *Materials & Design,* Vol. 32, pp. 3328-3335, 2011.

[23] ZERBST, U., VORMWALD, M., PIPPAN, R., GÄNSER, H.-P., SARRAZIN-BAUDOUX, C., MADIA, M.: About the fatigue crack propagation threshold of metals as a design criterion – A review, *Engineering Fracture Mechanics*, Vol. 153, pp. 190-243, 2016. 43, 2016.

Review process
Single-blind peer review process.